

# Kinesin spindle protein (KSP) inhibitors. Part 1: The discovery of 3,5-diaryl-4,5-dihydropyrazoles as potent and selective inhibitors of the mitotic kinesin KSP

Christopher D. Cox,<sup>a,\*</sup> Michael J. Breslin,<sup>a</sup> Brenda J. Mariano,<sup>a</sup> Paul J. Coleman,<sup>a</sup> Carolyn A. Buser,<sup>b</sup> Eileen S. Walsh,<sup>b</sup> Kelly Hamilton,<sup>b</sup> Hans E. Huber,<sup>b</sup> Nancy E. Kohl,<sup>b</sup> Maricel Torrent,<sup>c</sup> Youwei Yan,<sup>d</sup> Laurence C. Kuo<sup>d</sup> and George D. Hartman<sup>a</sup>

<sup>a</sup>Department of Medicinal Chemistry, Merck Research Laboratories, PO Box 4, Sumneytown Pike, West Point, PA 19486, USA

<sup>b</sup>Department of Cancer Research, Merck Research Laboratories, PO Box 4, Sumneytown Pike, West Point, PA 19486, USA

<sup>c</sup>Department of Molecular Systems, Merck Research Laboratories, PO Box 4, Sumneytown Pike, West Point, PA 19486, USA

<sup>d</sup>Department of Structural Biology, Merck Research Laboratories, PO Box 4, Sumneytown Pike, West Point, PA 19486, USA

Received 25 January 2005; revised 16 February 2005; accepted 17 February 2005

Available online 19 March 2005

**Abstract**—Optimization of high-throughput screening (HTS) hits resulted in the discovery of 3,5-diaryl-4,5-dihydropyrazoles as potent and selective inhibitors of KSP. Dihydropyrazole **15** is a potent, cell-active KSP inhibitor that induces apoptosis and generates aberrant mitotic spindles in human ovarian carcinoma cells at low nanomolar concentrations. X-ray crystallographic evidence is presented which demonstrates that these inhibitors bind in an allosteric pocket of KSP distant from the nucleotide and microtubule binding sites.

© 2005 Elsevier Ltd. All rights reserved.

## 1. Introduction

Small molecule inhibitors of KSP (kinesin spindle protein) represent a novel antimetabolic approach for the treatment of cancer. KSP, also known as *Hs* Eg5, is a member of the kinesin superfamily of molecular motors that utilize the energy generated from the hydrolysis of ATP to transport vesicles, organelles, and microtubules.<sup>1</sup> Inhibition of KSP prevents normal bipolar spindle formation, which leads to mitotic arrest with a characteristic monoastrial phenotype<sup>2,3</sup> and subsequently to apoptosis in transformed cells. The promise of designing a small molecule inhibitor of KSP that does not suffer from the solubility, neurotoxicity, and resistance profile limitations of the currently employed antimetotics led to our interest in developing a KSP inhibitor (KSPi) for the treatment of cancer.<sup>4</sup>

We describe herein the discovery of potent and selective 3,5-diaryl-4,5-dihydropyrazole inhibitors of KSP that were identified from optimization of high-throughput screening (HTS) hits. Dihydropyrazole **15** is a potent, cell-active KSPi that induces apoptosis and generates aberrant mitotic spindles in human ovarian carcinoma cells at low nanomolar concentrations. Additionally, we show X-ray crystallographic evidence that these inhibitors bind in an allosteric pocket of KSP distant from the nucleotide and microtubule binding sites.

## 2. Chemistry

A medicinal chemistry effort to find small molecule inhibitors of KSP was initiated following HTS of our in-house sample collection. The primary screen that we utilized to determine potency is an *in vitro* ATPase assay measuring the test compound's ability to prevent the hydrolysis of ATP to ADP in the presence of microtubules, thus providing a measure of enzyme inhibition.<sup>5</sup> 3,5-Diaryl-4,5-dihydropyrazoles **1** and **2** (Fig. 1) stood out as promising hits from the initial screen. Interestingly, the lack of potency in the unsubstituted analog

**Keywords:** KSP; Mitotic kinesins; Anti-metotics; Dihydropyrazoles.

\*Corresponding author. Tel.: +1 215 652 2411; fax: +1 215 652 7310; e-mail: [chris\\_cox@merck.com](mailto:chris_cox@merck.com)

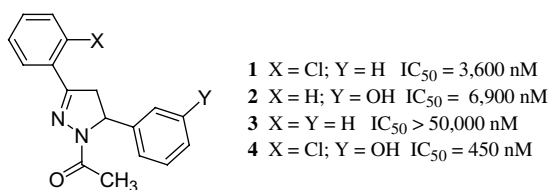
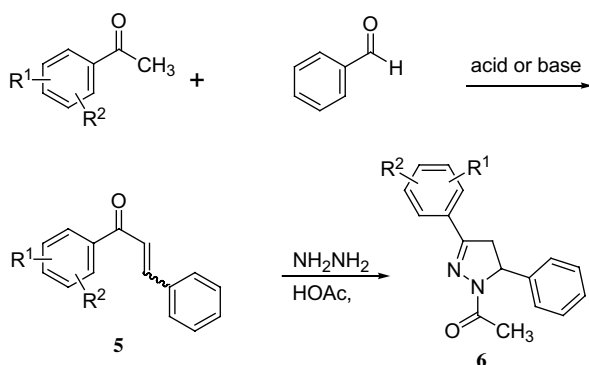


**Figure 1.** 3,5-Diaryl-4,5-dihydropyrazole inhibitors of KSP.



**Scheme 1.** Synthesis of *N*-acetyl-3,5-diaryl-4,5-dihydropyrazoles.

**3** indicated that substitution on each ring was critical for activity. We therefore merged the substitution patterns from the eastern ring of **1** and the western ring of **2** to provide **4** with a substantial boost in potency, quickly providing us with a sub-micromolar inhibitor of KSP.

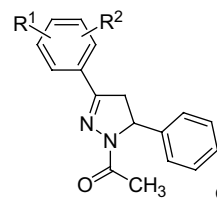
Synthesis of compounds in the 3,5-diaryl-4,5-dihydropyrazole series began with condensation of an aceto-phenone and an aromatic aldehyde to provide chalcone **5** (Scheme 1). Treatment of **5** with hydrazine in the presence of acetic acid provided target dihydropyrazole **6**, most likely by a sequence involving hydrazone formation followed by intramolecular conjugate addition and then acylation.<sup>6</sup> The promising early result with potent KSPi **4**, in conjunction with a facile synthesis commencing from readily available starting materials, encouraged us to explore the structure–activity relationship (SAR) of compounds in this series.

### 3. In vitro SAR

Utilizing **1** as a starting point, we began the optimization process by investigating the substitution pattern on the western aryl ring (Table 1). Whereas exchange of chlorine for fluorine was tolerated as demonstrated by **6a**, other modest modifications such as bromo, methyl, methoxy, and trifluoromethyl (**6b–e**) resulted in substantial losses in potency. The 3-chlorophenyl derivative **6f** was somewhat less potent relative to **1**, whereas the 4-chloro analog was inactive (**6g**).

Attempts to substitute the western aryl ring with polar substituents, or to replace the ring with a heterocycle, resulted in significant losses in potency relative to halo-

**Table 1.** SAR of the western aryl group of **6**<sup>a</sup>



Compound	R <sup>1</sup>	R <sup>2</sup>	ATPase (nM)
<b>6a</b>	2-F	H	3600
<b>6b</b>	2-Br	H	23,300
<b>6c</b>	2-CH <sub>3</sub>	H	46,200
<b>6d</b>	2-OCH <sub>3</sub>	H	>50,000
<b>6e</b>	2-CF <sub>3</sub>	H	>50,000
<b>6f</b>	3-Cl	H	9800
<b>6g</b>	4-Cl	H	>50,000
<b>6h</b>	2-F	3-F	12,700
<b>6i</b>	2-Cl	4-Cl	37,600
<b>6j</b>	2-F	6-F	10,900
<b>6k</b>	3-F	5-F	>5000 <sup>b</sup>
<b>6l</b>	2-F	5-F	94

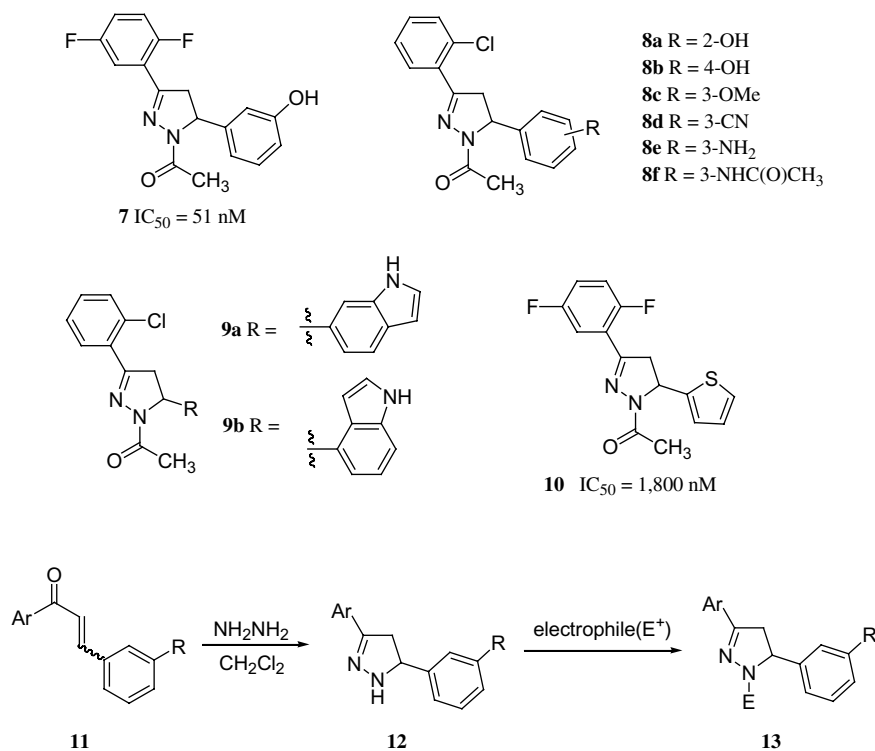
<sup>a</sup> All values reported are an average for *n* = 3 or greater. The standard deviation limits are generally within 25–50% of the reported values.

<sup>b</sup> This compound did not provide good titrations, possibly due to solubility issues; however, all results (*n* = 15) were >5000 nM.

genated analogs; however, a breakthrough was uncovered upon dihalogenation of the western ring. Whereas the 2,3-, 2,4-, 2,6-, and 3,5-dihalogenated analogs **6h–k** were uniformly less active than the best monohalogenated analogs, the 2,5-difluoro derivative **6l**, with an IC<sub>50</sub> = 94 nM, displayed an impressive 40-fold boost in potency relative to **1**. At this point we incorporated the 3-hydroxyl functionality on the eastern ring and were pleased to observe an additive effect: **7** inhibited KSP with an IC<sub>50</sub> = 51 nM.

We investigated in a parallel fashion the substitution pattern on the eastern aryl ring; unfortunately, this effort proved to be less fruitful, with no modifications providing improvement over the 3-hydroxyl substituent identified earlier. For example, moving the hydroxyl group to the 2- or 4-position (**8a,b**), or replacing the 3-hydroxyl group with 3-methoxy (**8c**), substantially reduced activity. Other hydrogen-bond donating and accepting groups, including those commonly thought of as phenol replacements,<sup>7</sup> provided analogs that were also less active than the parent (**8d–f**, **9a,b**). Additionally, we investigated heterocyclic and alkyl replacements for the eastern aryl group; disappointingly, no compounds inhibited ATPase activity below 10 μM with the exception of thiophene analog **10**, which had an IC<sub>50</sub> = 1.8 μM.

A third area of the molecule readily probed by a parallel synthesis approach was the N1-substituent of the 4,5-dihydropyrazole core. To access such structures, chalcones **11** were treated with hydrazine in dichloromethane and the resulting intermediate **12** was trapped with an electrophilic agent (Scheme 2). A variety of N1-substituted dihydropyrazoles **13** were prepared in this manner.<sup>8</sup>



**Scheme 2.** Synthesis of N1-substituted 3,5-diaryl-4,5-dihydropyrazoles **13**.

The SAR of N1-substitution is presented in Table 2. Increasing the size of the acyl group from acetyl to propionyl or isobutyryl (**13a,b**) led to analogs with reduced potency relative to **4**, but the original activity was restored in pivaloyl analog **13c**. The addition of polar functionality to a straight-chain alkyl substituent had a detrimental effect on potency (**13d**), as did benzoyl substitution (**13e**). Replacement of acetyl with methyl (**13f**)<sup>9</sup> or the addition of an oxygen spacer to provide a

methyl carbamate (**13g**) each resulted in a loss of measurable activity.

Continuing to investigate the SAR at N1, we changed to the more potent difluoro-substituted series with **6l** as a benchmark and found that thioacetyl analog **14a** provided a modest loss in potency, whereas the sulfonamide **14b** and monomethyl urea **14c** resulted in a more drastic loss. The activity contained in **6l** was restored in dimethyl urea **14d**.

**Table 2.** SAR of the N1-acyl group in 3,5-diaryl-4,5-dihydropyrazoles **13** and **14**<sup>a</sup>

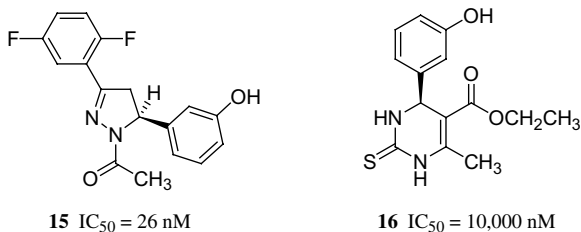
Compound	E	ATPase (nM)
<b>13a</b>	C(O)CH <sub>2</sub> CH <sub>3</sub>	1200
<b>13b</b>	C(O)CH(CH <sub>3</sub> ) <sub>2</sub>	1100
<b>13c</b>	C(O)C(CH <sub>3</sub> ) <sub>3</sub>	460
<b>13d</b>	C(O)(CH <sub>2</sub> ) <sub>3</sub> NH <sub>2</sub>	6000
<b>13e</b>	C(O)Ph	13,500
<b>13f</b>	Me	>50,000
<b>13g</b>	C(O)OMe	>50,000
<b>14a</b>	C(S)CH <sub>3</sub>	250
<b>14b</b>	SO <sub>2</sub> Me	1800
<b>14c</b>	C(O)NHMe	3100
<b>14d</b>	C(O)NMe <sub>2</sub>	84

<sup>a</sup> See footnote a in Table 1.

#### 4. Mechanistic and X-ray crystallographic studies

We chose **7** as a tool to further our understanding of the mechanism of KSP inhibition by compounds in the 3,5-diaryl-4,5-dihydropyrazole series. Resolution of the enantiomers of **7** by chiral stationary phase HPLC revealed that the KSP activity resided only in the (*S*)-antipode **15**, which had an IC<sub>50</sub> = 26 nM.<sup>10</sup> Counter-screening across a panel of eight structurally and functionally related mitotic and transport kinesins indicates that **15** is >2000-fold selective for KSP.<sup>11</sup> Additionally, inhibition of KSP by **15** is not competitive with either ATP or microtubules, suggesting an allosteric mode of action wherein the binding site of the inhibitor is remote from both the nucleotide and microtubule binding sites. Finally, we found that **15** does not affect tubulin polymerization in vitro at 20 μM,<sup>12</sup> distinguishing it mechanistically from the taxanes.

We recently described the 1.9 Å resolution structure of the ternary complex of the motor domain of KSP, **16**, and Mg-ADP.<sup>13</sup> From this structure, we discovered



that the inhibitor occupies an ‘induced fit’ pocket 12 Å removed from the nucleotide binding site that is not present in the apo-structure, and creates widespread structural changes throughout the protein. We have now solved a similar structure of KSP-4-ADP at 2.5 Å.<sup>14</sup>

The active site of the KSP-4-ADP complex is pictured in Figure 2, overlaid with the KSP-16-ADP active site described previously. 4,5-Dihydropyrazole **4** induced very similar gross structural changes in the protein, and, as predicted by computer-generated docking models, occupied the same binding site as **16**. The inhibitors share two common features upon binding. First, both possess a hydrogen-bonding interaction between the phenolic hydroxyl group and the carbonyl oxygen of the backbone amide bond of Glu118 (2.7 Å in **16**, 2.5 Å in **4**). Secondly, each displays a hydrophobic interaction between the aromatic ring of the phenol and the induced nonpolar pocket. However, the main difference in the two structures is the ability of the chlorophenyl group of **4** to effectively fill a large hydrophobic pocket not utilized by the less potent inhibitor **16**. Also of note is the fact that the N1-acyl group of **4** rests in a solvent exposed area of the binding site.

These structural features nicely explain the SAR and mechanistic observations made above: (1) though racemic **4** was used for soaking, only the (*S*)-antipode bound to the enzyme;<sup>15</sup> (2) 3-hydroxy substitution on the eastern aryl ring was uniquely potency enhancing; (3) re-

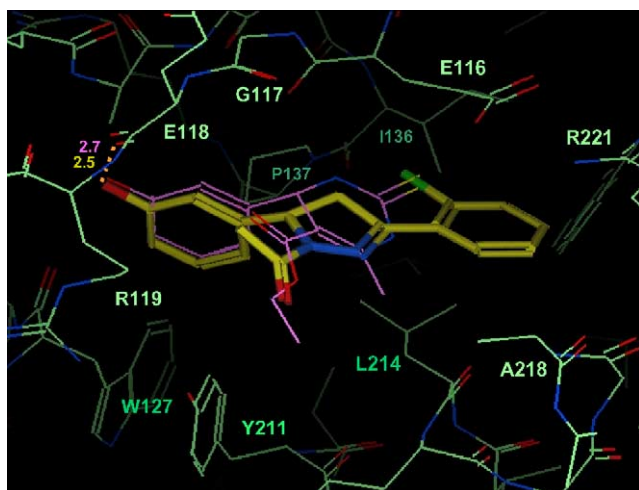


**Figure 2.** Overlay of the X-ray structures of KSP-4-ADP (yellow) and KSP-16-ADP (pink). The H-bond from the phenolic hydroxyl group of each inhibitor to Glu118 is highlighted.

moval of either aryl group, or replacement with a polar heterocycle, led to a reduction in potency due to the loss of favorable hydrophobic interactions; (4) the acyl group is close to a solvent exposed area and thus helps account for the greater structural diversity tolerated in this portion of the molecule; (5) the inhibitor binding site is well-removed from the nucleotide and microtubule binding sites, and so explains the lack of competition with ATP and microtubules; and (6) loop L5 in KSP folds inward to trap the inhibitor in the induced binding site in the ternary structure, whereas L5 is flexible and solvent exposed in the apo-structure.<sup>13</sup> Sequence alignment of the motor domain of over 100 kinases from nine different subfamilies reveals that the primary sequence of L5 is unique to the motor domain of KSP and helps explain the exquisite selectivity of our inhibitors.

## 5. Cell activity

A cell-based assay measuring caspase-3 activation, a well-known marker of apoptosis, was carried out with **15** to appraise its ability to enter and kill cells.<sup>16</sup> In good agreement with the ATPase results disclosed above, caspase-3 induction occurred in A2780 human ovarian carcinoma cells with an IC<sub>50</sub> = 15 nM. Additionally, we found that A2780 cells incubated in the presence of **15** (100 nM) displayed the characteristic monoaster phenotype,<sup>5</sup> thus providing support for KSP inhibition as the trigger of apoptosis.

## 6. Conclusion

We described a novel series of compounds based on the 3,5-diaryl-4,5-dihydropyrazole scaffold that are potent and selective inhibitors of the mitotic kinesin KSP. Beginning from a high-throughput screen, we were able to rapidly identify KSP inhibitors with potency in the low nanomolar range that possess favorable physical and biological properties. We used these compounds to gain functional and structural insight into the mechanism of inhibition. Dihydropyrazole **15** has an IC<sub>50</sub> = 26 nM for inhibition of KSP, a log *P* of 3.1, and a molecular weight of only 316. It is believed that further structural modifications to optimize pharmacokinetics and ancillary activities will lead to clinical candidates for the treatment of cancer.

## Acknowledgments

We thank Ms. Yi Yang and Ms. Yun Zhang for performing the cell-based analysis of **15**.

## References and notes

- (a) Sharp, D. J.; Rogers, G. C.; Scholey, J. M. *Nature* **2000**, *407*, 41; (b) Mandelkow, E.; Mandelkow, E.-M. *Trends Cell Biol.* **2002**, *12*, 585; (c) Endow, S. A.; Baker, D. S. *Annu. Rev. Physiol.* **2003**, *65*, 161.

2. (a) Mayer, T. U.; Kapoor, T. M.; Haggarty, S. J.; King, R. W.; Schreiber, S. L.; Mitchison, T. J. *Science* **1999**, *286*, 971; (b) Kapoor, T. M.; Mayer, T. U.; Coughlin, M. L.; Mitchison, T. J. *J. Cell Biol.* **2000**, *150*, 975.
3. Sakowicz, R.; Finer, J. T.; Beraud, C.; Crompton, A.; Lewis, E.; Fritsch, A.; Lee, Y.; Mak, J.; Moody, R.; Turincio, R.; Chabala, J. C.; Gonzales, P.; Roth, S.; Weitman, S.; Wood, K. W. *Cancer Res.* **2004**, *64*, 3276.
4. For an overview of the mitotic spindle as target for cancer therapeutics, see: (a) Wood, K. W.; Cornwell, W. D.; Jackson, J. R. *Curr. Opin. Pharmacol.* **2001**, *0*, 370; For kinesin-targeted therapeutics, see: (b) Wood, K. W.; Bergnes, G. *Ann. Rep. Med. Chem.* **2004**, *39*, 173.
5. The biological assays utilized herein have been described; see: (a) Breslin, M. J.; Coleman, P. J.; Cox, C. D.; Culberson, C. J.; Hartman, G. D.; Mariano, B. J.; Torrent, M. PCT WO 03/079973 A2, 2003; (b) Ref. 13.
6. For example synthetic procedures, see: (a) Safak, C.; Tayhan, A.; Sarac, S.; Yulug, N. *J. Indian Chem. Soc.* **1990**, *67*, 571; (b) Ref. 5a.
7. Asselin, A. A.; Humber, L. G.; Crosilla, D.; Oshiro, G.; Wojdan, A.; Grimes, D.; Heaslip, R. J.; Rimele, T. J.; Shaw, C.-C. *J. Med. Chem.* **1986**, *29*, 1009.
8. A similar synthetic approach has previously been taken in a parallel solution phase library synthesis; see: Bauer, U.; Egner, B. J.; Nilsson, I.; Berghult, M. *Tetrahedron Lett.* **2000**, *41*, 2713.
9. Dihydropyrazole **13f** can be easily accessed by heating chalcone in the presence of methylhydrazine in EtOH at 80 °C for 2 h.
10. Separation of 500 mg of **7** was carried out on a 250 × 5 cm 20 μM Chiralpak AD column with 80% hexanes (modified with 0.1% TFA) and 20% EtOH at 75 mL/min. The first isomer to elute, the (+) antipode, was 'inactive' (IC<sub>50</sub> = 4.1 μM). The second isomer to elute, the (–) antipode, was active (IC<sub>50</sub> = 26 nM). Each isomer was ≥99% ee by analytical HPLC under the same conditions. Data for **15**: [α]<sub>D</sub><sup>20</sup> –88.9 (c 3.5, MeOH). NMR (500 MHz, DMSO-*d*<sub>6</sub>): δ 9.4 (s, 1H), 7.7 (m, 1H), 7.4 (m, 2H), 7.1 (m, 1H), 6.7–6.5 (m, 3H), 5.4 (m, 1H), 3.9 (m, 1H), 3.1 (m, 1H), 2.3 (s, 3H) ppm. HRMS (ES) calcd M+H for C<sub>17</sub>H<sub>14</sub>F<sub>2</sub>N<sub>2</sub>O<sub>2</sub>: 317.1096. Found 317.1105. See Ref. 15 for assignment of absolute stereochemistry as *S*.
11. The IC<sub>50</sub>'s of KSPi **15** when tested against the motor domains of eight additional kinesins (CENP-E, MKLP-1, Kif3A, Kif1B, uKHC, nKHC, KIF14, and MCAK) were greater than 50 μM in ATPase assays similar to that described for KSP. The selection of these counter-screens was based on considerations of homology and function.
12. The effect of **15** on the polymerization of tubulin was measured by turbidity (optical density at 340 nm) in 96-well plates at 37 °C in a SpectroMax Ultra (modified from Lopes, N. M.; Miller, H. P.; Young, N. D.; Bhuyan, B. K. *Cancer Chemother. Pharmacol.* **1997**, *41*, 37). KSPi **15** and control compounds (taxol and colchicine) were resuspended in DMSO and diluted to 20 μM in 1× buffer (80 mM K-PIPES, 1 mM EGTA, 1 mM MgCl<sub>2</sub>, pH 6.8) containing 1 mM GTP. The assay was initiated by adding cold tubulin at 2.5 mg/mL to each well (to a total volume of 200 μL; 1% final DMSO).
13. Yan, Y.; Sardana, V.; Xu, B.; Homnick, C.; Halczenko, W.; Buser, C. A.; Schaber, M.; Hartman, G. D.; Huber, H. E.; Kuo, L. C. *J. Mol. Biol.* **2004**, *335*, 547.
14. Co-crystals of the ternary complex of KSP-ADP(Mg<sup>2+</sup>)-monastrol were first formed with the vapor diffusion method (see Ref. 13). The KSP monastrol ternary crystals then soaked in the harvest solution (28% PEG3350, 0.2 M K<sub>2</sub>HPO<sub>4</sub> at pH 8.0) containing 2 mM **4** for 2 days to replace monastrol at the inhibitor binding site. The X-ray diffraction data were collected at 100 K at synchrotron beamline 17-ID of the Advanced Photon Source at Argonne National Laboratory to 2.5 Å resolution in the space group P2<sub>1</sub>2<sub>1</sub>2<sub>1</sub> with cell dimensions of *a* = 69.3 Å, *b* = 79.8 Å, and *c* = 159.6 Å (*R*<sub>sym</sub> = 0.066 and completeness = 94%). The ternary complex structure of KSP-4-ADP(Mg<sup>2+</sup>) was determined by the use of the difference Fourier method and refined to an *R*-factor of 0.25. The coordinates have been deposited with RCSB Protein Data Bank under the accession code 1YRS.
15. We have solved the crystal structure of the ternary complex of KSP, ADP and over 20 structurally-related inhibitors. In each case, only the *S*-antipode was found to bind in the active site. The absolute stereochemistry of **14** was assigned by analogy.
16. Caspase-3 activity in cell lysates was determined using the ApoAlert Caspase-3 fluorescent assay kit (Clontech, Palo Alto, CA), which measures the release of the 7-amino-4-trifluoromethylcoumarin (AFC) fluorophore from the substrate DEVD-AFC.